LIMNOLOGY and OCEANOGRAPHY

ASLO

Limnol. Oceanogr. 65, 2020, 2158–2169

doi: 10.1002/lno.11445

Concentration and isotopic composition of mercury in a blackwater river affected by extreme flooding events

Martin Tsz-Ki Tsui,[1*] **Habibullah Uzun**,[2,3] **Alexander Ruecker**,[4,5] **Hamed Majidzadeh**,[4,6] **Yener Ulus**,[1] **Hongyuan Zhang**,[7] **Shaowu Bao**,[7] **Joel D. Blum**,[8] **Tanju Karanfil**,[2] **Alex T. Chow**[4]

[1]Department of Biology, University of North Carolina at Greensboro, Greensboro, North Carolina
[2]Department of Environmental Engineering and Earth Sciences, Clemson University, Clemson, South Carolina
[3]Department of Environmental Engineering, Marmara University, Istanbul, Turkey
[4]Biogeochemistry and Environmental Quality Research Group, Clemson University, Georgetown, South Carolina
[5]Department of Biogeochemical Processes, Max Planck Institute for Biogeochemistry, Jena, Germany
[6]Department of Sciences, Southern New Hampshire University, Manchester, New Hampshire
[7]Department of Coastal and Marine Systems Science, Coastal Carolina University, Conway, South Carolina
[8]Department of Earth and Environmental Sciences, University of Michigan, Ann Arbor, Michigan

Abstract

Torrential rain and extreme flooding caused by Atlantic hurricanes mobilize a large pool of organic matter (OM) from coastal forested watersheds in the southeastern United States. However, the mobilization of toxic metals such as mercury (Hg) that are associated with this vast pool of OM are rarely measured. This study aims to assess the variations of total Hg (THg) and methylmercury (MeHg) levels and the isotopic compositions of Hg in a blackwater river (Waccamaw River, SC, U.S.A.) during two recent extreme flooding events induced by Hurricane Joaquin (October 2015) and Hurricane Matthew (October 2016). We show that extreme flooding considerably increased filtered THg and MeHg concentrations associated with aromatic dissolved organic matter. During a 2-month sampling window each year (October–November), we estimate that about 27% (2015) and 78% (2016) of the average amount of Hg deposited atmospherically during these 2 months was exported via the river. The isotopic composition of Hg in the river waters was changed only slightly by the substantial inputs of runoff from surrounding landscapes, in which mass-dependent fractionation (as δ^{202}Hg) decreased from −1.47 to −1.67‰ and mass-independent fractionation (as Δ^{199}Hg) decreased from −0.15 to −0.37‰. The slight variations in Hg isotopic composition during such extreme flooding events imply that sources of Hg in the river are nearly unchanged even under the very high wet deposition of Hg derived from the intensive rainfall. The majority of Hg exported by the river (74–85%) is estimated to have been derived from dry deposition to the watersheds. An increase in frequency and intensity of Atlantic hurricanes is expected in the next few decades due to further warming of ocean surface waters. We predict that increased hurricanes will mobilize more dry-deposited Hg and in situ produced MeHg from these coastal watersheds where MeHg can be extensively bioaccumulated and biomagnified in the downstream aquatic food webs.

Blackwater rivers are common in the topographically flat coastal plain along the Atlantic coast in the southeastern United States, spanning from southern Virginia to Florida. These rivers drain a landscape with extensive forested wetlands, swamps, and marshes. River water is often dark brown with high levels of dissolved organic carbon (DOC) up to ~ 50 mg C L^{-1} (Smock et al. 2005). Levels of DOC can be greatly altered by extreme weather events in the region such as Atlantic tropical storms and hurricanes, which are severe societal threats and influence the coastal plain in late summer and fall. Partly attributed to global warming of the sea surface, it is anticipated that the frequency of Atlantic hurricanes of category 3 or higher will increase significantly by the end of this century (Bender et al. 2010). The formation of strong tropical hurricanes can cause extensive rainfall in a short period of time leading to extreme flooding in the coastal plain (Feaster et al. 2015).

Besides damage to infrastructure and property, extreme flooding can greatly alter biogeochemical cycling of many important chemical constituents. For example, three times higher mobilization of DOC and dissolved organic nitrogen in years of extreme flooding have been found, compared to prior years, in the lower coastal plain of South Carolina due to two

*Correspondence: tmtsui@uncg.edu

Additional Supporting Information may be found in the online version of this article.

recent powerful hurricanes; Hurricane Joaquin in 2015 and Hurricane Matthew in 2016 (Majidzadeh et al. 2017). Other more recent extreme events in the coastal plain of the Carolinas were caused by Hurricane Florence in 2018 and Hurricane Dorian in 2019. Thus, the occurrence of powerful hurricanes in the late summer and fall on the Atlantic coastal plain is becoming more routine, and their biogeochemical consequences warrant better characterization.

In addition to inputs of carbon and nitrogen, there is concern for the mobilization of toxic metals such as mercury (Hg), because Hg transport is tightly coupled to dissolved organic matter (DOM) in surface water through binding to thiol groups (Ravichandran 2004). Extreme flooding may mobilize a large quantity of atmospherically deposited inorganic Hg (as Hg(II)) and highly toxic methylmercury (MeHg) produced under the reducing conditions within coastal plain wetland systems (Guentzel 2009). However, direct sampling of surface water and measurements for Hg in systems under extreme flooding conditions are rarely conducted. Thus, it is important to quantify the fluvial export of total Hg (THg) and MeHg from these coastal plain watersheds under extreme flooding events. Nearly all of these rivers carry fish consumption advisories for Hg (South Carolina Department of Health and Environmental Control [SCDHEC] 2018), which are triggered in South Carolina at tissue concentration > 0.25 μg g^{-1} wet wt.

It is important to understand the quantity of Hg exported by blackwater rivers and whether there are shifts in the sources of Hg exported by these rivers during extreme flooding events (Bradley et al. 2010). The sources of Hg can be fingerprinted by examining the isotopic compositions of Hg in environmental samples (Tsui et al. 2020). There are seven naturally occurring Hg isotopes with varying abundance: ^{196}Hg, ^{198}Hg, ^{199}Hg, ^{200}Hg, ^{201}Hg, ^{202}Hg, and ^{204}Hg. It is well established that Hg isotopes can undergo mass-dependent fractionation (MDF), commonly expressed as δ^{202}Hg, via many different redox reactions, and Hg isotopes can also undergo large-magnitude mass-independent fractionation (MIF or "odd-MIF"), commonly expressed as Δ^{199}Hg or Δ^{201}Hg, via photochemical reactions including photoreduction of Hg(II) and photodemethylation of MeHg. In addition, even-mass Hg isotopes, that is, ^{200}Hg and ^{204}Hg, can undergo small but significant magnitude MIF called "even-MIF," commonly expressed as Δ^{200}Hg or Δ^{204}Hg, due to photochemical reactions in the upper atmosphere (Chen et al. 2012; Blum and Johnson 2017). Odd-MIF is mediated by the magnetic isotope effect (MIE) or nuclear volume effect (NVE), with the ratio of Δ^{199}Hg/Δ^{201}Hg being diagnostic of the mechanism causing odd-MIF, that is, a ratio of Δ^{199}Hg/Δ^{201}Hg $\sim$ 1.0 for MIE (Bergquist and Blum 2007) and $\sim$ 1.5–1.6 for NVE (Zheng and Hintelmann 2010; Ghosh et al. 2013).

Recent studies measuring the natural abundance of Hg stable isotope ratios have shown that the source(s) of Hg in surface water can be constrained by examining the isotopic composition of aqueous Hg. Both MDF and odd-MIF can vary depending on the hydrological conditions and atmospheric deposition of Hg in the watersheds (Jiskra et al. 2017; Woerndle et al. 2018). Thus, Hg isotope analyses may potentially help distinguish changes in the source(s) of Hg during extreme flooding events in blackwater river ecosystems if water sampling is conducted during the period of rapid changes in river hydrographs (Phillips and Slattery 2007; Majidzadeh et al. 2017).

In this work, we aimed to better understand biogeochemical Hg cycling in blackwater river ecosystems under extreme flooding events. We hypothesized that hurricane-induced extreme flooding would lead to (1) significantly higher riverine fluxes of THg and MeHg, and (2) an increasing proportion of aqueous Hg in the river derived from Hg that was wet deposited onto the system, that is, Hg(II) derived from intensive rainfall. We tested these hypotheses using concentration and isotopic analyses in the Waccamaw River, which drains the lower coastal plain of South Carolina, and is a representative blackwater river of the Atlantic coast with widespread fish consumption advisories for Hg (South Carolina Department of Health and Environmental Control [SCDHEC] 2018). Our sampling was conducted during and after flooding events in the coastal area following landfall of two Atlantic hurricanes in two consecutive years in early October in 2015 (Hurricane Joaquin) and in 2016 (Hurricane Matthew).

Materials and methods

Field sampling

We sampled at two locations along the Waccamaw River: WaccaWache Landing in Murrells Inlet, SC (MI site; 33°33′42.77″N, 79°5′11.61″W; drainage area: 41,623 km^2) and Bay Road Landing in Socastee, SC (ST site; 33°40′5.06″N, 79°3′39.90″W; drainage area: 4317 km^2) (Supporting Information Fig. S1). Vegetated landscapes make up $\sim$ 88% and $\sim$ 93% of the surface area in the basin for the MI site and the ST site, respectively (Supporting Information Table S1 and Fig. S2). In 2015, intense rainfall began on 01 October and continued through 05 October resulting in total rainfall exceeding 500 mm in coastal areas (Feaster et al. 2015), with peak discharge at both sampling sites occurring on 08 October 2015. Overall, we collected 12 sets of surface-water samples at each site from 05 October 2015 to 30 November 2015 and our sampling covered the rising limb, peak discharge, and falling limb of the river hydrograph in 2015.

In 2016, the duration of the intensive rainfall event was much shorter ($\sim$ 1 d), but with much higher intensity on 08 October 2016, which resulted in a total amount of precipitation lower than in 2015. Immediately following the hurricanes, the high cumulative rainfall near the coastal areas spread further inland in 2016 compared to 2015 (Supporting Information Fig. S3), causing much higher peak discharge in the river at the MI site in 2016 (Supporting Information Fig. S4). Our team started sampling 2 d after the peak rainfall on 10 October 2016 when the river discharge was already at

its peak, and thus our sampling covered mainly the peak discharge and the falling limb of the river hydrograph in 2016, generating 12 sets of water samples at each site from 10 October 2016 to 26 November 2016.

All surface-water samples were collected using a trace metal clean protocol in the field. Specifically, surface-water samples were collected into acid-cleaned 500 mL Nalgene Teflon bottles for total-Hg (THg) and MeHg analyses, and into clean 1-liter amber glass bottles for: DOC, specific UV absorbance at 254 nm ($SUVA_{254}$; as a proxy of DOC aromaticity; Weishaar et al. 2003), total dissolved nitrogen (TDN), and filtered total iron (Fe) analyses. On six selected dates along the river hydrograph in 2015 at the ST site, we also collected surface water into acid-cleaned 5-liter Pyrex borosilicate glass media bottles for Hg isotopic analyses, because a larger amount of Hg, for example, > 15 ng, is required for high-precision Hg isotopic measurements (Woerndle et al. 2018).

All water samples for Hg analyses were transported overnight on ice in a cooler to the analytical laboratory at the University of North Carolina at Greensboro (UNCG; Greensboro, NC, U.S.A.). All water samples were filtered and then either fully digested for THg and Hg isotope analysis following Woerndle et al. (2018) or preserved with hydrochloric acid for MeHg analysis (see details in Supporting Information Text S1). Water samples collected into amber glass bottles were sent on ice to an analytical laboratory at Clemson University (Anderson, SC, U.S.A.), where the samples were filtered through 0.45-μm prewashed filters, and analyzed for DOC, $SUVA_{254}$, TDN, and filtered total Fe (see details in Supporting Information Text S2).

Additional environmental samples (litter, surface soil, and fish) were collected to examine THg, MeHg (soil only), and the isotopic compositions of Hg (selected samples only) in the Waccamaw River and adjacent ecosystems. These additional samples were collected in 15–24 October 2016, 02–10 November 2016, and 02–03 May 2017 (see details in Supporting Information Text S3).

Mercury concentration and isotopic analyses

Concentrations of THg and MeHg were analyzed for all surface water, litter (THg only), fish fillet (THg only), and soil samples using a Brooks Rand Model III cold vapor atomic fluorescence spectrometer. Sample analyses were carried out with appropriate quality control and quality assurance procedures (see details in Supporting Information Text S4). Isotopic

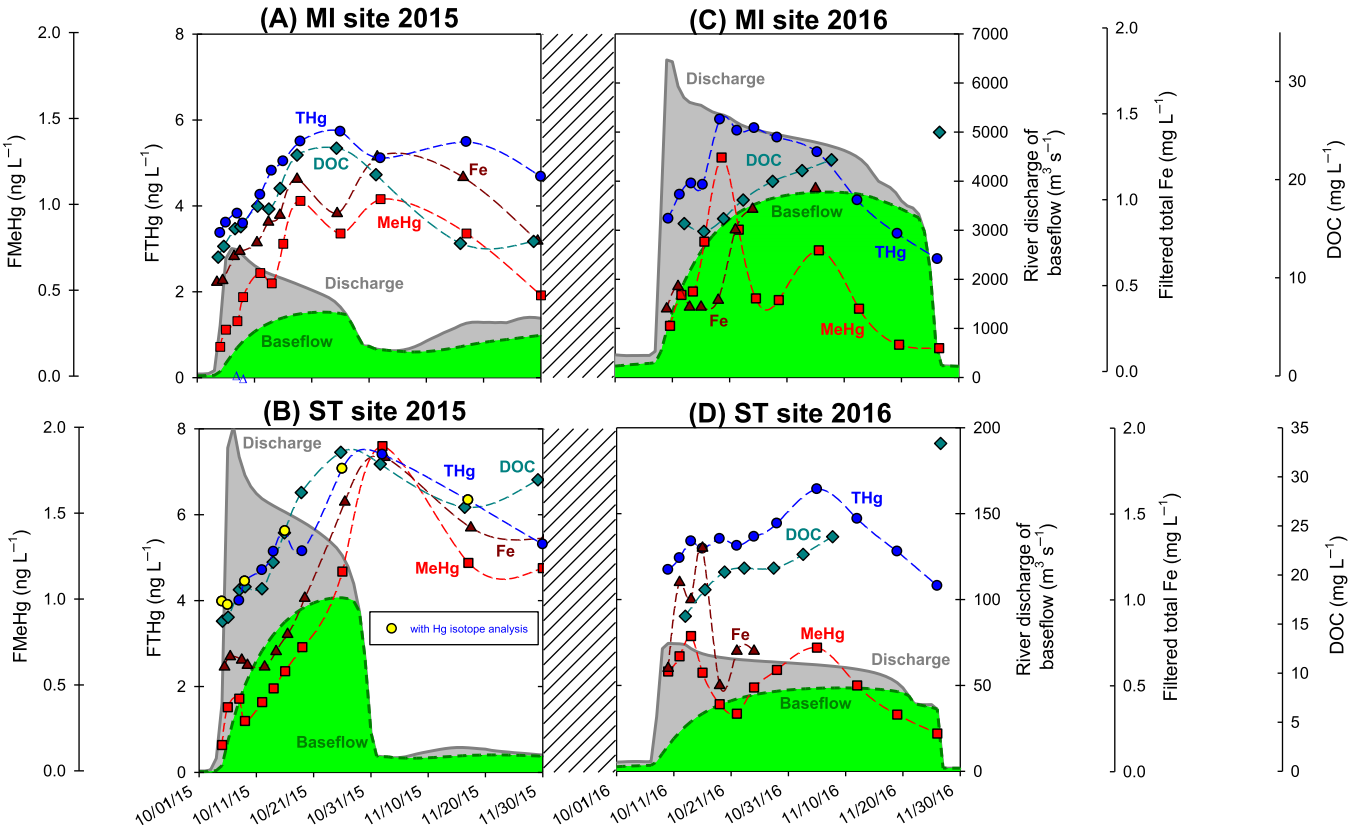

Fig. 1. Concentrations of filtered total-mercury (FTHg), filtered methylmercury (FMeHg), filtered total iron (Fe), dissolved organic carbon (DOC), river discharge, and estimated baseflow for the Waccamaw River in (**A**) 2015 October–November period at MI site (Murrells Inlet, SC), (**B**) 2015 October–November period at ST site (Socastee, SC), (**C**) 2016 October–November period at MI site, and (**D**) 2016 October–November period at ST site. Data for individual water samples can be found in Supporting Information Tables S2, S3. In panel (**B**), yellow filled circle denotes that the particular sample was also analyzed for Hg isotopic composition.

compositions of Hg in selected surface-water samples and environmental samples were processed at UNCG, and high precision Hg isotope analysis was carried out at the University of Michigan (Ann Arbor, MI, U.S.A.) using a Nu Instruments multicollector-inductively coupled plasma mass spectrometer (see details in Supporting Information Text S5).

Water quality data for the Waccamaw River

We retrieved hydrological and water quality data from a USGS gaging station (ID: 02110704) on the Waccamaw River (Conway, SC) about 20 km upstream from the ST site (URL: https://waterdata.usgs.gov/usa/nwis/uv?site_no=02110704) to illustrate how each hurricane impacted the water quality during the rising limb, peak discharge, and falling limb of the hydrograph. It should be noted that in 2016 the equipment measuring water quality at the gaging station was not functioning properly from 12 October through 02 November due to the extremely high water level in the river, and thus data are missing during this period.

Data analyses

Hydrological modeling was performed to calculate the river discharge and the proportion of runoff (overland flow) vs. baseflow at each sampling point (MI and ST) using a previously described method (Majidzadeh et al. 2017). Separation of flow into baseflow and surface runoff can potentially improve our understanding of changes in water chemistry. One would expect baseflow to respond to large precipitation events with a lag-time compared with surface flow (Simpson et al. 2013; Jazaei et al. 2017). This delayed response can have impacts on the contributing flow, fluxes, and water chemistry (Jazaei et al. 2017; Majidzadeh et al. 2017) including THg, MeHg, and the sources of Hg as potentially revealed by changes in Hg isotope compositions.

We estimated the daily export of THg during the monitoring period (October–November) in both 2015 and 2016, and compared the daily export with the averaged daily atmospheric deposition of Hg in the watershed, which we derived from a nearby Mercury Deposition Network (MDN) site in coastal South Carolina near Charleston, SC, U.S.A. (MDN site SC05; Risch et al. 2012). The available data from 2007 to 2009 indicated that combined dry (litterfall) and wet (rain) deposition of Hg was 17.5 μg m^{-2} yr^{-1}, and thus the averaged daily deposition of Hg was 0.048 μg m^{-2} d^{-1}. We calculated the daily watershed yield of THg and compared that to the averaged daily deposition of Hg to the watershed.

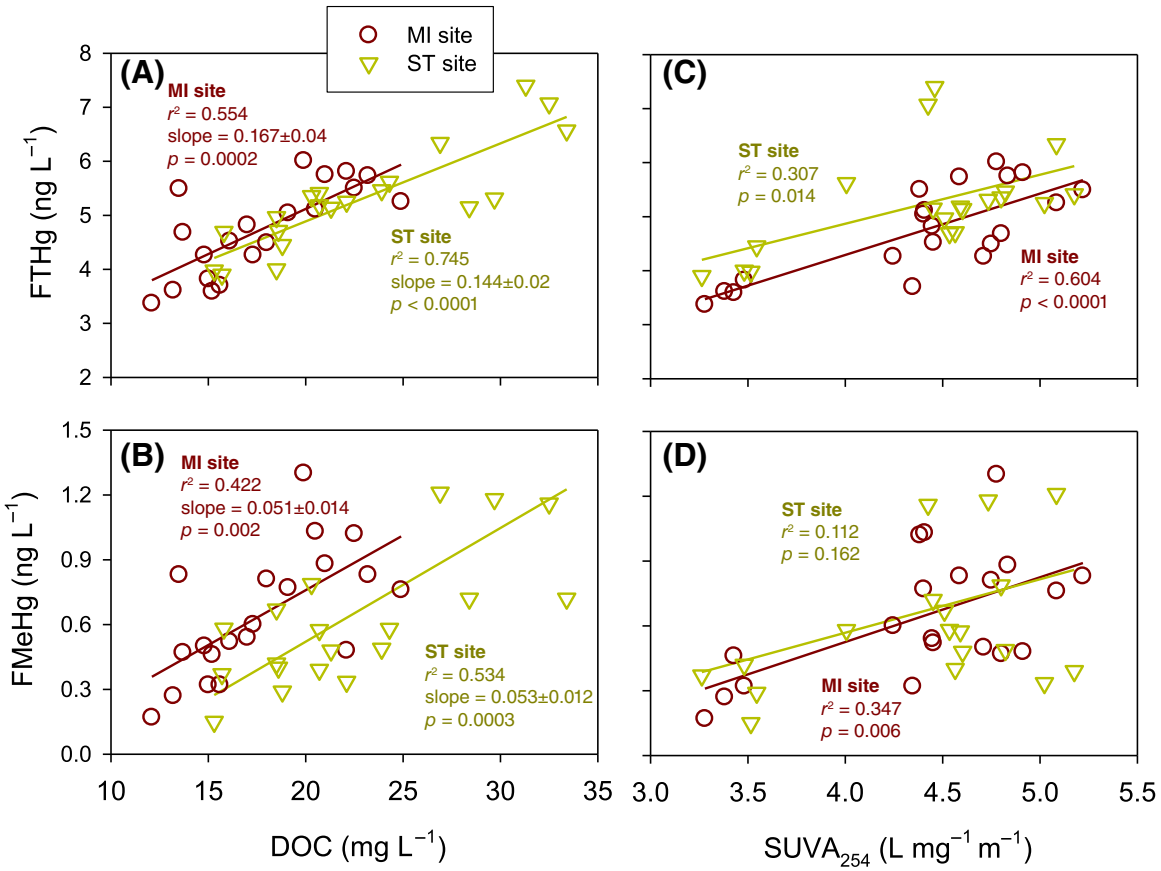

Fig. 2. Relationships between (**A**) dissolved organic carbon (DOC) and filtered total-mercury (FTHg), (**B**) DOC and filtered methylmercury (FMeHg), (**C**) specific UV absorbance at 254 nm (SUVA$_{254}$) and FTHg, and (**D**) SUVA$_{254}$ and FMeHg at both locations—MI site (Murrells Inlet, SC) and ST site (Socastee, SC).

To further explore the origin of Hg in surface water, we used a simple binary mixing equation to model δ^{202}Hg (MDF) values (Woerndle et al. 2018). As end-members, we used the Hg isotopic compositions of forest floor litter to estimate dry deposition (mean ± SD: −1.93 ± 0.072‰; n = 3) and precipitation measurements from the literature to estimate wet deposition (mean ± SD: 0.05 ± 0.134‰; n = 21). Mercury isotopic values of precipitation are from previous studies in Florida (Sherman et al. 2012) and California (Donovan et al. 2013). It should be noted that the application of the simple end-member mixing model does not take into account possible fractionation processes that may take place in the soil and water, for example, Hg(II) reduction and re-emission.

For all data, linear regression analyses were performed using SigmaPlot 12.5; the data passed the normal distribution test (Shapiro–Wilk) indicating that they are not severely skewed. The significance level for all statistical analyses was set at α = 0.05.

Results

River discharge and water parameters as impacted by extreme flooding

Due to the much larger drainage basin for the MI site (41,623 km^2) compared to the ST site (4317 km^2), the river discharge at the MI site was much higher in both years (Supporting Information Fig. S4). The peak discharge was also delayed a few days after the heavy rainfall in both years. From the USGS gaging station at ~ 20 km upstream of the ST site, the water quality data showed that the Waccamaw River did not become depleted in dissolved oxygen (DO) before or after the peak of the hydrograph. In both years, it is clear that DO levels sharply increased with the increasing river discharge (Supporting Information Fig. S5A,B), but DO levels dropped to a level lower than the preflooded period and finally DO levels returned to higher values as flow decreased. Specific conductance of the river water also significantly decreased with the peak of the river hydrograph (Supporting Information Fig. S5C,D) while the turbidity of the river increased sharply due to the inputs of surface runoff from the surrounding vegetated landscape (Supporting Information Fig. S5E,F). The pH decreased slightly with increase in river discharge (Supporting Information Fig. S5G,H). Water temperature declined over time during the sampling period in both 2015 and 2016, as air temperature decreased and subsurface (baseflow) inputs with lower temperature increased during the later part of the river hydrograph (Supporting Information Fig. S5I,J). Thus, these rapid changes in the water quality data illustrate the temporal impacts of extreme flooding on the river system and yield clues to the potential flow paths of the floodwaters.

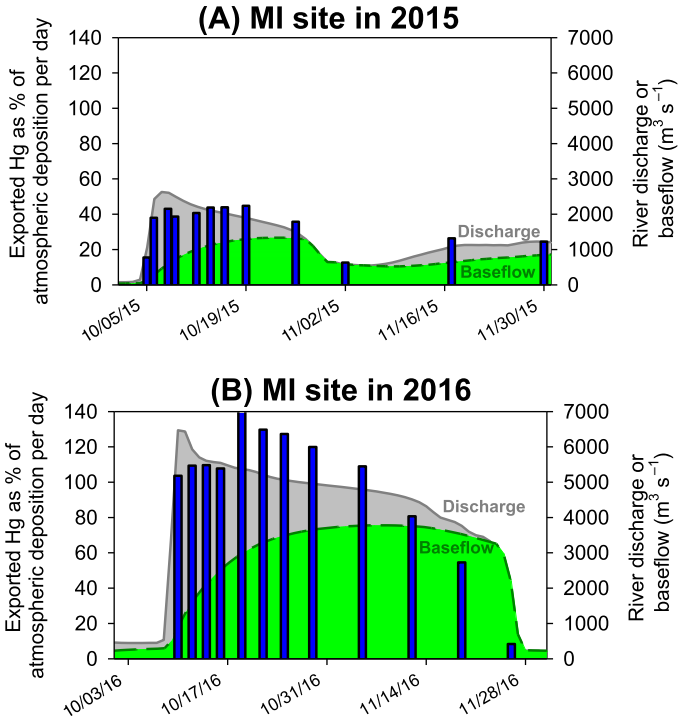

Fig. 3. Calculated percentage of the average daily deposited Hg (wet and dry) in the watershed that was exported by the river at the MI site (Murrells Inlet, SC) in the study period (October–November) in (**A**) 2015 and (**B**) 2016. Both graphs include river discharge (gray solid line) and baseflow (green dashed line).

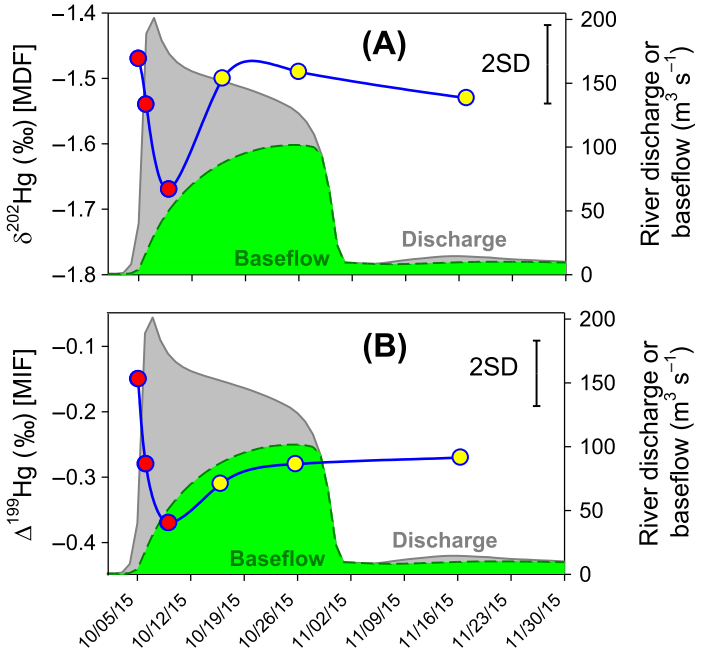

Fig. 4. Isotopic compositions of mercury (Hg) in filtered river water: (**A**) mass-dependent fractionation (MDF) (as δ^{202}Hg) and (**B**) mass-independent fractionation (MIF) (as Δ^{199}Hg), at ST site (Socastee, SC) in 2015 October–November sampling period (in circle symbols with blue line; separated into those collected in rising limb and peak in red, and falling limb in yellow). Error bars represent external analytical reproducibility (2SD) of Hg isotope measurements in this study. The isotope data for water samples can be found in Supporting Information Table S5. The graphs also include the river discharge (gray dashed line) and estimated baseflow (green dashed line).

Fluctuations of DOC and mercury

At both sampling sites in both years, the baseflow increased on the rising limb, peak, and the initial phase of the falling limb of the hydrographs, and over the increase of baseflow both DOC (12.1–23.2 mg L^{-1} at MI site; 15.3–32.5 mg L^{-1} at ST site) and filtered total Fe (0.52–1.25 mg L^{-1} at MI site; 0.61–1.83 mg L^{-1} at ST site) increased sharply, especially at both sites in 2015 (Fig. 1). Similarly, there were concurrent increases in FTHg (3.37–5.73 ng L^{-1} at MI site; 3.98–7.40 ng L^{-1} at ST site) and FMeHg (0.14–1.02 ng L^{-1} at MI site; 0.15–1.89 ng L^{-1} at ST site) when baseflow increased (Fig. 1; Supporting Information Tables S2, S3).

There were, however, delayed responses in the first peak of FTHg relative to the peak discharge especially for the ST site, that is, 18 and 22 d for MI and ST sites in 2015, respectively; 9 d and 25 d for MI and ST sites in 2016, respectively. There were similar, but more subtle, delayed responses for FMeHg, that is, 12 d and 26 d for MI and ST sites in 2015, respectively; 9 d

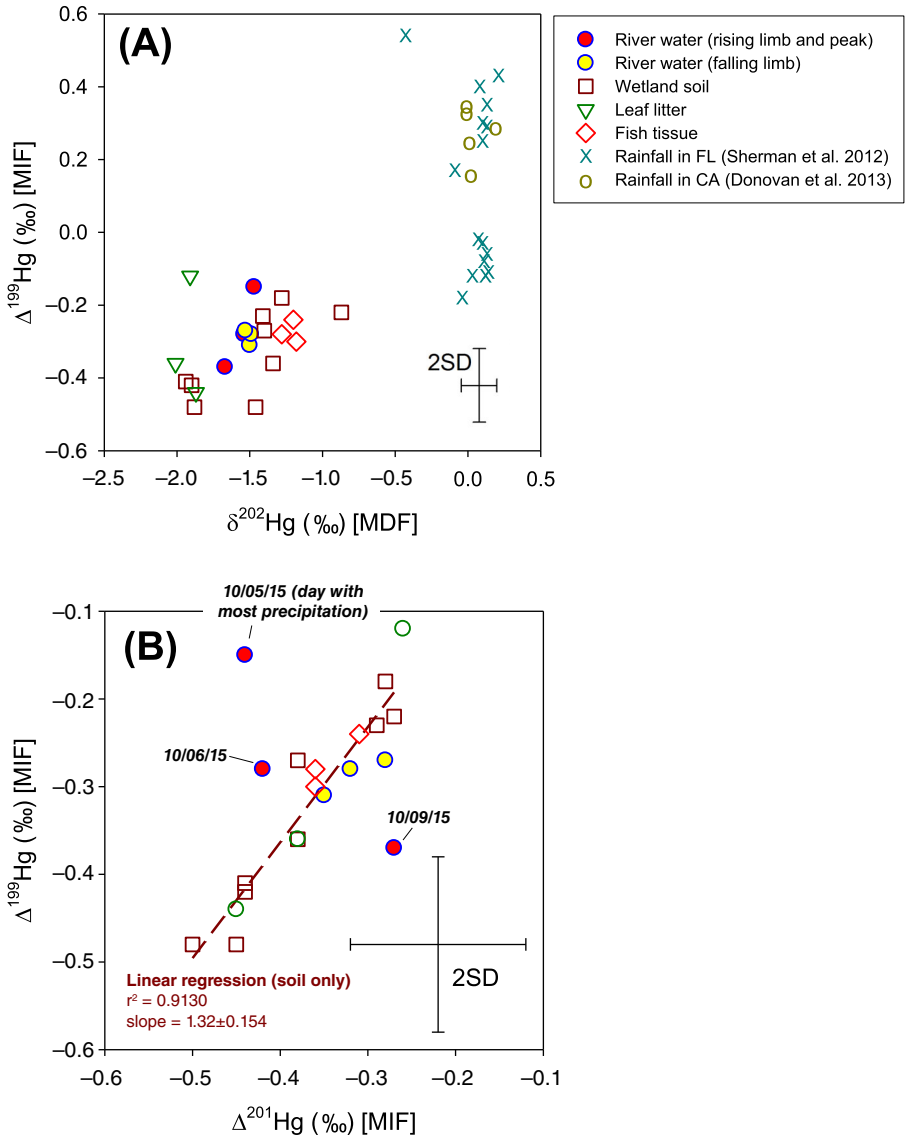

Fig. 5. (**A**) Isotopic compositions of mercury (Hg) in all samples from this study: mass-dependent fractionation (MDF) (as δ^{202}Hg) and mass-independent fractionation (MIF) (as Δ^{199}Hg), of filtered river water samples (separated into those collected in rising limb and peak in red, and falling limb in yellow) at the ST site (Socastee, SC) in 2015 October–November sampling period. Also shown are the Hg isotope compositions of litter samples (n = 3), soil samples (n = 9), and fish tissue samples (n = 3) from the study system (see their sampling locations in Supporting Information Fig. S1 and Table S4). The isotopic compositions of Hg from precipitation (distant from point sources) in two previous studies in Florida (FL) and California (CA) are also included (Sherman et al. 2012; Donovan et al. 2013). (**B**) Relationship between Δ^{201}Hg and Δ^{199}Hg (both are MIF of odd-mass Hg isotopes) among different types of samples collected in this study. Error bars in both panels show typical external analytical reproducibility (2SD) of Hg isotope measurements from this study. The isotopic data for water samples and environmental samples can be found in Supporting Information Tables S5, S6, respectively.

and 4.5 d for MI and ST sites in 2016, respectively (Fig. 1). There was also a positive and significant correlation for both FTHg and FMeHg with DOC and $SUVA_{254}$ with p values ranging from < 0.0001 to 0.014, with the exception of the correlation between FMeHg and $SUVA_{254}$ at the ST site with $p = 0.162$ (Fig. 2).

Mobilization of atmospherically deposited mercury by extreme flooding

In October–November 2015, the river exported FTHg at a rate of up to ~ 40% of average daily atmospheric deposition of Hg (Fig. 3A) while in 2016 the percentage exceeded 100% on the falling limb of the river hydrograph when FTHg concentrations were elevated (Fig. 3B). Thus, based on these two extreme flooding events, we find that increased flooding and river discharge can export large amounts of atmospherically deposited Hg from the watershed. The daily river export rate exceeded the daily atmospheric deposition rate for short periods of time in 2016. Over the 2-month monitoring period (October–November) for each of 2 yr, there was one extreme flooding event. During these 2 month periods, the river exported a mean of ~ 27% in October–November 2015 and ~ 78% in October–November 2016 of the Hg estimated to have been atmospherically deposited in the watershed during these 2-month periods.

The highest daily export of MeHg (3.98 ng m^{-2} d^{-1} in 2015 and 14.5 ng m^{-2} d^{-1} in 2016) occurred during the falling limb of the river hydrograph in both years, or about 2 weeks after the peak discharge was achieved (Supporting Information Fig. S6). The daily export of MeHg was much more elevated during 2016 when river discharge was significantly higher at the MI site than in 2015. Over the 2-month (October–November) monitoring period, the MeHg export normalized to watershed area in October–November 2015 and 2016 was 0.12 μg m^{-2} and 0.28 μg m^{-2}, respectively.

Soil samples collected along the Waccamaw River and adjacent ecosystems showed wide ranges of THg and MeHg, and more importantly, there were significant ($p < 0.0001$), positive correlations between organic matter (OM) content (measured as loss-on-ignition [LOI]) and both THg and MeHg concentrations (Supporting Information Fig. S7). Fish fillet samples exhibited high THg concentrations, which were 891 ng g^{-1} dry-wt. for bluegill ($n = 1$), 2125 ng g^{-1} dry wt. for yellow perch ($n = 1$), and 2220 ng g^{-1} dry wt. for warmouth ($n = 1$).

Isotopic compositions of mercury in river water and environmental samples

Overall, there were only very limited ranges in values for both δ^{202}Hg (range: −1.67 to −1.47‰) and Δ^{199}Hg (range: −0.37 to −0.15‰) among the six water samples analyzed, even though river discharge varied by more than a factor of 20 (8.6–211 m^3 s^{-1}) during the 6-week sampling period in 2015 at the ST site (Fig. 4 and Supporting Information Table S5). Both δ^{202}Hg (before: −1.47‰; after: −1.67‰) and Δ^{199}Hg (before: −0.15‰; after: −0.37‰) declined right after the peak discharge was reached on 06 October 2015. In contrast to the narrow range in Hg isotope values observed in river water, larger ranges of MDF but not MIF were found among the surface soil samples (δ^{202}Hg: −1.94 to −0.87‰; Δ^{199}Hg: −0.48 to −0.18‰; $n = 9$) collected in wetlands and forested landscapes along the Waccamaw River (Fig. 5A and Supporting Information Table S6). Three litter samples exhibited a narrow range in δ^{202}Hg (−2.01 to 1.87‰) and Δ^{199}Hg (−0.44 to −0.12‰) while three fish fillet samples, each of a different species, displayed almost identical values of δ^{202}Hg (−1.28 to −1.18‰) and Δ^{199}Hg (−0.30 to −0.24‰) (Fig. 5A and Supporting Information Table S6). The Δ^{199}Hg values of THg in fish fillets were slightly negative, similar to the Δ^{199}Hg values found in the litter, soil, and water samples. On a plot of Δ^{199}Hg vs. Δ^{201}Hg, soil samples exhibited a $\Delta^{199}Hg/\Delta^{201}Hg$ ratio of 1.32 ± 0.15, while three water samples collected during the rising limb and peak discharge showed values deviating from the positive relationship between Δ^{199}Hg and Δ^{201}Hg (Fig. 5B). The small variations of MIF of Hg isotopes among different compartments (i.e., litter, wetland soils, river water, and fish) suggest that dry deposition of Hg through foliage uptake of gaseous elemental Hg represents the dominant source of Hg to these coastal watersheds while photochemical processes (e.g., MeHg photodemethylation) are minimal in this blackwater river ecosystem.

The binary mixing model reveals that ~ 78% of Hg in river water was derived from dry deposition (range: 74–85% over the 6-weeks sampling period) while ~ 76% (range: 40–100%) of soil Hg from our sampling sites was derived from dry deposition.

Discussion

This study is based on sampling of river water during and after two extreme flooding events in the low-lying Atlantic coastal plain where there is high Hg methylation potential due to the presence of extensive wetlands (Guentzel 2009) and where there are widespread fish consumption advisories against Hg (South Carolina Department of Health and Environmental Control [SCDHEC] 2018). Blackwater river ecosystems are hotspots for MeHg production and bioaccumulation, and the range of Hg in the Waccamaw River reported here (FTHg: 2.76–7.40 ng L^{-1}; FMeHg: 0.17–1.89 ng L^{-1}; $n = 48$ including both sites) is similar to concentrations found in other blackwater river ecosystems in the low-lying Atlantic coastal plain. For example, Brigham et al. (2009) monitored and reported FTHg (2.14–14.20 ng L^{-1}; $n = 38$) and FMeHg (< 0.04–1.03 ng L^{-1}; $n = 37$) in the St. Marys River along the state border of Georgia and Florida from 2002 to 2006. Many of these blackwater river ecosystems can be severely affected by Atlantic hurricanes and the associated extreme flooding events, and thus our research results can potentially be applied to the understanding of Hg cycling in other Atlantic coastal watersheds under the threat of extreme flooding events.

Rapid changes in water chemistry during extreme flooding events

In both years, the peak discharge was delayed after the intense rainfall, indicating that surface runoff occurred first

while precipitation started to infiltrate into the vegetated landscapes before recharging groundwater systems and then enhancing surface water discharge (Majidzadeh et al. 2017). Although the nearest USGS gaging station was located about 20 km upstream of our sampling sites on the Waccamaw River, the water quality data (Supporting Information Fig. S5) are valuable for demonstrating the dynamic nature and the impacts of extreme flooding on water quality parameters as driven by changes in flow path (i.e., runoff vs. baseflow). The rapid increase of river discharge during the initial phase of extreme flooding elevated DOC, filtered total Fe, FTHg, and FMeHg levels (Fig. 1), which are likely driven by the increasing proportion of river flow from baseflow. This result is consistent with the finding of a previous study in the coastal plain showing that the major source of stream water and Hg is from groundwater or baseflow during nonflooded periods (Bradley et al. 2010).

The changes in Hg isotopic compositions of river water during the 6-week sampling period at the ST site in 2015 support the conclusion stated above that substantial inputs of surface runoff significantly decreased both δ^{202}Hg (before: −1.47‰; after: −1.67‰) and Δ^{199}Hg (before: −0.15‰; after: −0.37‰) in surface water (Fig. 4). This isotopic change occurred because surface runoff contains mobilized Hg previously dry deposited into the watershed with different isotopic compositions of Hg from the baseflow as demonstrated in a previous study on a small peatland catchment (Woerndle et al. 2018), in which the authors reported higher δ^{202}Hg values in the baseflow (-1.41 ± 0.07‰; $n = 3$) than in the surface streamflow (-1.83 ± 0.17‰; $n = 24$) but no differences in Δ^{199}Hg values (baseflow: -0.26 ± 0.03‰; $n = 3$; streamflow: -0.25 ± 0.07‰; $n = 24$). When baseflow returned to be the dominant river flow, both δ^{202}Hg and Δ^{199}Hg values in river water returned to higher values, which we assume to be closer to the isotopic composition of Hg in groundwater, although we did not directly sample groundwater in this study. Overall, the variation of Hg isotope compositions in river water in this study is quite small compared to the small catchment study discussed above that examined Hg isotope variation over 2 yr in water flowing from a headwater upland-peatland catchment in northern Minnesota (Woerndle et al. 2018). In the catchment study, δ^{202}Hg varied more widely from −2.12 to −1.32‰ under different hydrological conditions, while Δ^{199}Hg varied to a similar extent as in this study from −0.35 to −0.12‰ over 2 yr of monitoring (Woerndle et al. 2018).

Transport and sources of mercury in rivers

Positive relationships between FTHg and FMeHg with DOC have been observed in numerous fluvial Hg studies (Balogh et al. 2008; Brigham et al. 2009; Schuster et al. 2011; Tsui and Finlay 2011; Bravo et al. 2018; Lavoie et al. 2019) because DOM is presumed to be the dominant carrier of inorganic Hg and MeHg in surface water through complexation with thiol groups (Ravichandran 2004).

The reported ratios between FTHg and DOC (0.144–0.167 ng mg^{-1}) and between FMeHg and DOC (0.051–0.053 ng mg^{-1}) in this study of the Waccamaw River are similar to other lake and river studies in the North America that were recently compiled by Lavoie et al. (2019) and for which the ratio between FTHg and DOC was found to be 0.30 ± 0.19 ng mg^{-1} (compiled from 31 studies on 1973 samples) and the ratio between FMeHg and DOC was found to be 0.045 ± 0.06 ng mg^{-1} (compiled from 20 studies on 1068 samples). These relationships suggest similar binding capacities of DOC to THg and MeHg in watersheds across a large geographic gradient. Furthermore, $SUVA_{254}$ positively correlated with FTHg and FMeHg at both sites (Fig. 2), suggesting that hydrologic flow paths through forested wetland soils late in the river hydrograph can mobilize large pools of aromatic DOM associated with elevated FTHg and FMeHg after extreme flooding, when baseflow becomes the dominant water source to surface water during the falling limb of the river hydrograph (Fig. 2).

Mercury isotopic compositions of filtered river water were within the larger range of Hg isotopic compositions of surface soil samples (Fig. 5A), suggesting that a mixture of different soil types and horizons could represent the main source of Hg to the river water. However, under different flow paths such as runoff vs. baseflow, the exact source(s) of Hg can vary. It should be noted that mobilization of Hg associated with DOM can occur through the release of DOM-Hg complexes from soil OM without inducing additional MDF (Jiskra et al. 2017). The binary mixing model results show that Hg in soil and river water is mainly derived from previous dry deposition into the watersheds, which is consistent with other studies in vegetated ecosystems examining both soil (Demers et al. 2013; Enrico et al. 2016; Obrist et al. 2017) and surface-water samples (Jiskra et al. 2017; Woerndle et al. 2018).

Fluxes of mercury and methylmercury

It should be noted that our estimation of fluvial export of Hg was based on filtered THg analyses, which we believe is appropriate because most of the Hg is in the dissolved phase in this blackwater river ecosystem even during high flow periods (e.g., > 80%; Guentzel 2009). Thus, we assume that our estimate would only be 10–20% higher if we considered both filtered and particulate fractions of THg. We also note that if extrapolating Hg fluxes to the entire year, the impact of a single extreme flooding event on annual export of atmospherically deposited Hg could be significant. We did not quantify the annual export because we did not collect samples for Hg analysis outside the October–November monitoring window in either year. However, our seasonal estimates (Fig. 3) demonstrate the large magnitude of fluvial Hg transport for a few weeks after major hurricanes, and the THg export would be further elevated when larger areas of the basin are impacted (e.g., 2016), resulting in higher river discharge and fluvial fluxes of Hg.

The MeHg export values during extreme flooding conditions (i.e., 2-month export of filtered MeHg: 0.24 μg m^{-2} in 2015 and 0.88 μg m^{-2} in 2016) are considerably higher than those estimated by a previous study of the Waccamaw River under both high and moderate discharges (e.g., 2-month export of filtered MeHg: < 0.07 μg m^{-2}; Guentzel 2009), illustrating the further elevation of MeHg export during extreme flooding events in these coastal watersheds. These export values for MeHg over just a 2-month period of very high flow are still considerably higher than those estimated for annual MeHg export from other studied rivers in the southeastern United States (e.g., Santa Fe River, FL; Brigham et al. 2009) in which investigators found 2-month watershed yields for MeHg to be just 0.031 μg m^{-2} under normal flow conditions. However, we expect that during extreme flooding in these low-lying systems, the watershed yield of MeHg would also be elevated considerably.

Further exploring MIF of mercury isotopes

As shown in Fig. 5B, there are small but discernible variations of MIF signatures (both Δ^{199}Hg and Δ^{201}Hg) among the samples analyzed in this study. Our observed ratio of Δ^{199}Hg/Δ^{201}Hg (1.32) among surface soil samples is very similar to the Δ^{199}Hg/Δ^{201}Hg ratio of 1.25 previously observed in Histosol samples from a boreal forest (Jiskra et al. 2015). Our sample size (n = 9) is somewhat small but the data may indicate that abiotic dark reduction of Hg can be important in these forested wetland ecosystems based on our measured Δ^{199}Hg/Δ^{201}Hg ratio, which is intermediate between the ratios of odd-MIF generated by MIE (1.0) and NVE (1.5–1.6). This observation warrants more detailed sampling and analyses to test the hypothesis that NVE fractionation of Hg is occurring in the saturated surface soils in the extensive wetland ecosystems of the coastal plain. For river water samples, it is interesting to note that among the three samples on the rising limb and at the peak of the river hydrograph (Fig. 5B) their Δ^{199}Hg/Δ^{201}Hg ratios do not fall on the linear trend defined by the other samples. Such deviations in Δ^{199}Hg/Δ^{201}Hg ratios have not been observed previously and seem unlikely to be attributable to analytical uncertainty. We suggest that this should be further explored in the future with higher frequency sampling and Hg isotope analysis of river water and precipitation throughout hurricane landfalls.

Sources and transformations of methylmercury in blackwater river ecosystem

It is well known that MeHg is the most toxic form of Hg as it can extensively bioaccumulate and biomagnify in natural food webs (Lavoie et al. 2013; Tsui et al. 2019). In this river ecosystem study, mobilization of MeHg may enhance biological uptake in downstream river locations and estuaries (e.g., Winyah Bay; Guentzel and Tsukamoto 2001), and thus it is potentially a health concern that extreme flooding can mobilize a large quantity of MeHg from forested landscapes such as wetlands and swamps in the Atlantic coastal plain (Smock et al. 2005).

The surface soil samples exhibited wide ranges of THg and MeHg concentrations and OM content (Supporting Information Table S4). This represents a variability in potential sources of Hg to the river with varying degrees of soil OM decomposition, and this may lead to observed variations of MDF and MIF of Hg in the river water (Woerndle et al. 2018). Among all surface soil samples analyzed, both THg and MeHg levels increased significantly with increasing LOI or OM content (Supporting Information Fig. S7). This result suggests that organic-rich soils, which are especially abundant in forested wetlands in the Atlantic coastal plain (Chow et al. 2013), are important sources of THg and MeHg to the Waccamaw River; similar to rivers investigated in southern Louisiana and the Gulf of Mexico coastal areas (Hall et al. 2008). The ranges of MeHg in soils from this study are also similar to those found in coastal freshwater marshes near the mouth of the Mississippi River (with a mean of 4.2 ng g^{-1} dry wt.; Kongchum et al. 2006).

As expected for our study area, which has widespread fish consumption advisories for Hg (South Carolina Department of Health and Environmental Control [SCDHEC] 2018), THg concentrations (assuming > 90% of THg as MeHg; Bloom 1992) in fish fillets in the three fish samples we analyzed were quite high (from 891 to 2220 ng g^{-1} dry wt. for three fish fillet samples). Indeed, these fish THg values match well to the low end of those reported in an earlier USGS study on fish bioaccumulation of Hg in the Santee River basin (Brumbaugh et al. 2001) and also in the lower coastal plain of South Carolina to the south of the current study area. In this USGS study, THg in largemouth bass was reported to range from 2355 to 9015 ng g^{-1} dry wt. (or equivalent to 0.47–1.80 μg g^{-1} wet wt., which is well above the USEPA recommended guideline of 0.3 μg g^{-1} wet wt.; USEPA 2010).

Despite the limited number of fish samples analyzed in this study, the Hg isotopic compositions of these three different fish species are strikingly similar, with δ^{202}Hg in the narrow range from −1.28 to −1.18‰ and Δ^{199}Hg in the narrow range from −0.30 to −0.24‰ (n = 3) (Fig. 5A and Supporting Information Table S6). All three fish samples show slightly negative Δ^{199}Hg values that resemble those observed in river water (Δ^{199}Hg: −0.37 to −0.15‰; n = 6), soils (Δ^{199}Hg: −0.48 to −0.18‰; n = 9), and litter (Δ^{199}Hg: −0.44 to −0.12‰; n = 3) collected in this study. This implies that the bioaccumulated MeHg in fish is largely derived from Hg previously dry deposited to the watersheds, since wet-deposited Hg typically has near zero or positive odd-MIF (e.g., Δ^{199}Hg: −0.18 to 0.56‰; n = 16; Sherman et al. 2012; Δ^{199}Hg: 0.16–0.53‰; n = 5; Donovan et al. 2013). MeHg in this blackwater river ecosystem did not undergo extensive photoreduction of Hg(II) and/or photodemethylation of MeHg prior to biological uptake, as these photochemical processes would increase MIF values of the residual MeHg remaining in the water column of the river

(Bergquist and Blum 2007; Tsui et al. 2013). To our knowledge, there have only been a few reports in the literature of negative odd-MIF of MeHg found in biota. One recent study reported slightly negative odd-MIF (Δ^{199}Hg ranging from −0.28 to −0.20‰) in several soil-dwelling invertebrate species from a wetland habitat in Acadia National Park in Maine, U.S.A. (Tsui et al. 2018). Even though our study river system receives extensive sunlight due to the wide channel width, aqueous MeHg is highly "shielded" from photodegradation since UV radiation is highly attenuated by the high levels of DOM in blackwater rivers (Morris et al. 1995) and the associated forested wetland habitats. In contrast, much more MeHg photodemethylation occurs in aquatic systems with high water clarity with low turbidity and/or low DOM (Sherman and Blum 2013; Tsui et al. 2013).

In summary, our sampling of river water from a blackwater river ecosystem in the lower coastal plain of South Carolina during two extreme flooding events showed a dynamic pattern of changes in THg and MeHg concentrations and fluvial exports. Subtle shifts in sources of Hg and MeHg from runoff to baseflow upon the reduction in river discharge following the storm events was observed with Hg isotope analysis of river water. We suggest that future studies should fully examine Hg biogeochemistry in these blackwater river ecosystems using measurements of Hg concentration and speciation as well as Hg stable isotopes. A greater understanding of the complexities of Hg cycling in the coastal plain ecosystem will aid in understanding why Hg methylation and bioaccumulation are highly elevated, and how the threat of increased Atlantic hurricane strength and extreme flooding will affect Hg biogeochemistry in these coastal river systems, which already have widespread fish consumption advisories for Hg.

References

Balogh, S. J., E. B. Swain, and Y. H. Nollet. 2008. Characteristics of mercury speciation in Minnesota rivers and streams. Environ. Pollut. **154**: 3–11. doi:10.1016/j.envpol.2007.11.014

Bender, M. A., T. R. Knutson, R. E. Tuleya, J. J. Sirutis, G. A. Vecchi, S. T. Garner, and I. M. Held. 2010. Modeled impact of anthropogenic warming on the frequency of intense Atlantic hurricanes. Science **327**: 454–458. doi:10.1126/science.1180568

Bergquist, B. A., and J. D. Blum. 2007. Mass-dependent and -independent fractionation of Hg isotopes by photoreduction in aquatic systems. Science **318**: 417–420. doi:10.1126/science.1148050

Bloom, N. S. 1992. On the chemical form of mercury in edible fish and marine invertebrate tissue. Can. J. Fish. Aquat. Sci. **49**: 1010–1017. doi:10.1139/f92-113

Blum, J. D., and M. W. Johnson. 2017. Recent developments in mercury stable isotope analysis. Rev. Mineral. Geochem. **82**: 733–757. doi:10.2138/rmg.2017.82.17

Bradley, P. M., C. A. Journey, F. H. Chapelle, M. A. Lowery, and P. A. Conrads. 2010. Flood hydrology and methylmercury availability in coastal plain rivers. Environ. Sci. Technol. **44**: 9285–9290. doi:10.1021/es102917j

Bravo, A. G., and others. 2018. The interplay between total mercury, methylmercury and dissolved organic matter in fluvial systems: A latitudinal study across Europe. Water Res. **144**: 172–182. doi:10.1016/j.watres.2018.06.064

Brigham, M. E., D. A. Wentz, G. R. Aiken, and D. P. Krabbenhoft. 2009. Mercury cycling in stream ecosystems. 1. Water column chemistry and transport. Environ. Sci. Technol. **43**: 2720–2725. doi:10.1021/es802694n

Brumbaugh, W. G., D. P. Krabbenhoft, D. R. Helsel, J. G. Wiener, and K. R. Echols. 2001. A national pilot study of mercury contamination of aquatic ecosystems along multiple gradients: Bioaccumulation in fish. USGS/BRD/BSR-2001-0009. U.S. Geological Survey.

Chen, J., H. Hintelmann, X. Feng, and B. Dimock. 2012. Unusual fractionation of both odd and even mercury isotopes in precipitation from Peterborough, ON, Canada. Geochim. Cosmochim. Acta **90**: 33–46. doi:10.1016/j.gca.2012.05.005

Chow, A. T., J. Dai, W. H. Conner, D. R. Hitchcock, and J. J. Wang. 2013. Dissolved organic matter and nutrient dynamics of a coastal freshwater forested wetland in Winyah Bay, South Carolina. Biogeochemistry **112**: 571–587. doi:10.1007/s10533-012-9750-z

Demers, J. D., J. D. Blum, and D. R. Zak. 2013. Mercury isotopes in a forested ecosystem: Implications for air-surface exchange dynamics and the global mercury cycle. Global Biogeochem. Cycles **27**: 222–238. doi:10.1002/gbc.20021

Donovan, P. M., J. D. Blum, D. Yee, G. E. Gehrke, and M. B. Singer. 2013. An isotopic record of mercury in San Francisco Bay sediment. Chem. Geol. **349/350**: 87–98. doi:10.1016/j.chemgeo.2013.04.017

Enrico, M., G. Le Roux, N. Marusczak, L. E. Heimbürger, A. Claustres, X. Fu, R. Sun, and J. E. Sonke. 2016. Atmospheric mercury transfer to peat bogs dominated by gaseous elemental mercury dry deposition. Environ. Sci. Technol. **50**: 2405–2412. doi:10.1021/acs.est.5b06058

Feaster, T. D., J. M. Shelton, and J. C. Robbins. 2015. Preliminary peak stage and streamflow data at selected USGS streamgaging stations for the South Carolina flood of October 2015, p. 19. U.S. Geological Survey Open-file Report 2015–1201. doi:10.3133/ofr20151201

Ghosh, S., E. A. Schauble, G. L. Couloume, J. D. Blum, and B. A. Bergquist. 2013. Estimation of nuclear volume dependent fractionation of mercury isotopes in equilibrium liquid-vapor evaporation experiments. Chem. Geol. **336**: 5–12. doi:10.1016/j.chemgeo.2012.01.008

Guentzel, J. L. 2009. Wetland influences on mercury transport and bioaccumulation in South Carolina. Sci. Total Environ. **407**: 1344–1353. doi:10.1016/j.scitotenv.2008.09.030

Guentzel, J. L., and Y. Tsukamoto. 2001. Processes influencing mercury speciation and bioconcentration in the North Inlet-

Winyah Bay Estuary, South Carolina, USA. Mar. Pollut. Bull. **42**: 615–619. doi:10.1016/S0025-326X(01)00090-X

Hall, B. D., G. R. Aiken, D. P. Krabbenhoft, M. Marvin-DiPasquale, and C. M. Swarzenski. 2008. Wetlands as principal zones of methylmercury production in southern Louisiana and the Gulf of Mexico region. Environ. Pollut. **154**: 124–134. doi:10.1016/j.envpol.2007.12.017

Jazaei, F., M. J. Simpson, and T. P. Clement. 2017. Understanding time scales of diffusive fluxes and the implication for steady state and steady shape conditions. Geophys. Res. Lett. **44**: 174–180. doi:10.1002/2016GL071914

Jiskra, M., J. G. Wiederhold, U. Skyllberg, R. M. Kronberg, I. Hajdas, and R. Kretzschmar. 2015. Mercury deposition and re-emission pathways in boreal forest soils investigated with Hg isotope signatures. Environ. Sci. Technol. **49**: 7188–7196. doi:10.1021/acs.est.5b00742

Jiskra, M., J. G. Wiederhold, U. Skyllberg, R.-M. Kronberg, and R. Kretzschmar. 2017. Source tracing of natural organic matter bound mercury in boreal forest runoff with mercury stable isotopes. Environ. Sci. Process. Impacts **19**: 1235–1248. doi:10.1039/C7EM00245A

Kongchum, M., I. Devai, R. D. DeLaune, and A. Jugsujinda. 2006. Total mercury and methylmercury in freshwater and salt marsh soils of the Mississippi river deltaic plain. Chemosphere **63**: 1300–1303. doi:10.1016/j.chemosphere.2005.09.024

Lavoie, R. A., T. D. Jardine, M. M. Chumchal, K. A. Kidd, and L. M. Campbell. 2013. Biomagnification of mercury in aquatic food webs: A worldwide meta-analysis. Environ. Sci. Technol. **47**: 13385–13394. doi:10.1021/es403103t

Lavoie, R. A., M. Amyot, and J.-F. Lapierre. 2019. Global meta-analysis on the relationship between mercury and dissolved organic carbon in freshwater environments. J. Geophys. Res. Biogeosci. **124**: 1508–1523. doi:10.1029/2018JG004896

Majidzadeh, M., and others. 2017. Extreme flooding mobilized dissolved organic matter from coastal forested wetlands. Biogeochemistry **136**: 293–309. doi:10.1007/s10533-017-0394-x

Morris, D. P., H. Zagarese, C. E. Williamson, E. G. Balseiro, B. R. Hargreaves, B. Modenutti, R. Moeller, and C. Queimalinos. 1995. The attenuation of solar UV radiation in lakes and the role of dissolved organic carbon. Limnol. Oceanogr. **40**: 1381–1391. doi:10.4319/lo.1995.40.8.1381

Obrist, D., and others. 2017. Tundra uptake of atmospheric elemental mercury drives Arctic mercury pollution. Nature **547**: 201–204. doi:10.1038/nature22997

Phillips, J. D., and M. C. Slattery. 2007. Downstream trends in discharge, slope, and stream power in a lower coastal plain river. J. Hydrol. **334**: 290–303. doi:10.1016/j.jhydrol.2006.10.018

Ravichandran, M. 2004. Interactions between mercury and dissolved organic matter – a review. Chemosphere **55**: 319–331. doi:10.1016/j.chemosphere.2003.11.011

Risch, M. R., J. F. DeWild, D. P. Krabbenhoft, R. K. Kolka, and L. Zhang. 2012. Litterfall mercury dry deposition in the eastern USA. Environ. Pollut. **161**: 284–290. doi:10.1016/j.envpol.2011.06.005

Schuster, P. F., R. G. Striegl, G. R. Aiken, D. P. Krabbenhoft, J. F. Dewild, K. Butler, B. Kamark, and M. Dornblaser. 2011. Mercury export from the Yukon River basin and potential response to a changing climate. Environ. Sci. Technol. **45**: 9262–9267. doi:10.1021/es202068b

Sherman, L. S., J. D. Blum, G. J. Keeler, J. D. Demers, and J. T. Dvonch. 2012. Investigation of local mercury deposition from a coal-fired power plant using mercury isotopes. Environ. Sci. Technol. **46**: 382–390. doi:10.1021/es202793c

Sherman, L. S., and J. D. Blum. 2013. Mercury stable isotopes in sediments and largemouth bass from Florida lakes, USA. Sci. Total Environ. **448**: 163–175. doi:10.1016/j.scitotenv.2012.09.038

Simpson, M. J., F. Jazaei, and T. P. Clement. 2013. How long does it take for aquifer recharge or aquifer discharge processes to reach steady state? J. Hydrol. **501**: 241–248. doi:10.1016/j.jhydrol.2013.08.005

Smock, L. A., A. B. Wright, and A. C. Benke. 2005. Atlantic coast of rivers of the southeastern United States. *In* A. C. Benke and C. E. Cushing [eds.], Rivers of North America. Elsevier p. 72–122.

South Carolina Department of Health and Environmental Control (SCDHEC). 2018. South Carolina fish consumption advisories Columbia, SC.

Tsui, M. T. K., and J. C. Finlay. 2011. Influence of dissolved organic carbon on methylmercury bioavailability across Minnesota stream ecosystems. Environ. Sci. Technol. **45**: 5981–5987. doi:10.1021/es200332f

Tsui, M. T. K., J. D. Blum, S. Y. Kwon, J. C. Finlay, S. J. Balogh, and Y. H. Nollet. 2013. Photodegradation of methylmercury in stream ecosystems. Limnol. Oceanogr. **58**: 13–22. doi:10.4319/lo.2013.58.1.0013

Tsui, M. T. K., E. M. Adams, A. K. Jackson, D. C. Evers, J. D. Blum, and S. J. Balogh. 2018. Understanding sources of methylmercury in songbirds with stable mercury isotopes: Challenges and future directions. Environ. Toxicol. Chem. **37**: 166–174. doi:10.1002/etc.3941

Tsui, M. T. K., and others. 2019. Controls of methylmercury bioaccumulation in forest floor food webs. Environ. Sci. Technol. **53**: 2434–2440. doi:10.1021/acs.est.8b06053

Tsui, M. T. K., J. D. Blum, and S. Y. Kwon. 2020. Review of stable mercury isotopes in ecology and biogeochemistry. Sci. Total Environ. **716**: 135386 doi:10.1016/j.scitotenv.2019.135386

USEPA. 2010. Guidance for implementing the January 2001 methylmercury water quality criterion. Office of Water. EPA-823-R-10-001. U.S. Environmental Protection Agency.

Weishaar, J. L., G. R. Aiken, B. A. Bergamaschi, M. S. Fram, R. Fujii, and M. Mopper. 2003. Evaluation of specific ultraviolet absorbance as an indicator of the chemical composition and reactivity of dissolved organic carbon. Environ. Sci. Technol. **37**: 4702–4708. doi:10.1021/es030360x

Woerndle, G. E., M. T. K. Tsui, S. D. Sebestyen, J. D. Blum, X. Nie, and R. K. Kolka. 2018. New insights on ecosystem

mercury cycling revealed by Hg isotopic measurements in water flowing from a headwater peatland catchment. Environ. Sci. Technol. **52**: 1854–1861. doi:10.1021/acs.est.7b04449

Zheng, W., and H. Hintelmann. 2010. Nuclear field shift effect in isotope fractionation of mercury during abiotic reduction in the absence of light. J. Phys. Chem. A **114**: 4238–4245. doi:10.1021/jp910353y

Acknowledgments

This study was supported by three National Science Foundation RAPID awards to the team (EAR-1617040, EAR-1711642, and CNS-1714015). We thank R. Oneal, R. Marsh, and S. Uzun (Clemson University) for their assistance in the field, and M. W. Johnson (University of Michigan) for his expert assistance with stable mercury isotope analysis. We also acknowledge S. J. Balogh (Metropolitan Council Environmental Services) who provided helpful comments on an earlier draft of this manuscript.

Conflict of Interest

None declared.

Submitted 24 April 2019
Revised 25 November 2019
Accepted 10 March 2020

Associate editor: Robert O. Hall